Articles

Solution Structure of the DNA Binding Domain of Rice Telomere Binding Protein RTBP1[†,‡]

Sunggeon Ko,[§] Eun Young Yu,[||] Joon Shin,[§] Hyun Hee Yoo,[||] Toshiyuki Tanaka,[⊥] Woo Taek Kim,[||] Hyun-Soo Cho,[||] Weontae Lee,*[,§] and In Kwon Chung*[,||]

Departments of Biochemistry and Biology, Protein Network Research Center, Yonsei University, Seoul 120-749, Korea, and Institute of Applied Biochemistry, University of Tsukuba, Tsukuba, Ibaraki 305-8572, Japan

Received July 7, 2008; Revised Manuscript Received December 20, 2008

ABSTRACT: RTBP1 is a rice telomeric protein that binds to the duplex array of TTTAGGG repeats at chromosome ends. The DNA binding domain of RTBP1 contains a Myb-type DNA binding motif and a highly conserved C-terminal Myb extension that is unique to plant telomeric proteins. Using an electrophoretic mobility shift assay, we identified the C-terminal 110-amino acid region ($RTBP1_{506-615}$) as the minimal telomeric DNA binding domain, suggesting that the Myb extension is required for binding plant telomeric DNA. Like other telomeric proteins such as human TRF1 and yeast Rap1, RTBP1 induced a DNA bending in the telomeric repeat sequence, suggesting that RTBP1 may play a role in establishing and/or maintaining an active telomere configuration in vivo. To elucidate the DNA binding mode of RTBP1, we determined the three-dimensional structure of $RTBP1_{506-615}$ in solution by NMR spectroscopy. The overall structure of $RTBP1_{506-615}$ is composed of four α-helices and stabilized by three hydrophobic patches. The second and third helices in RTBP1 form a helix−turn−helix motif that interacts directly with DNA. The fourth helix located in the Myb extension is essential for binding to telomeric DNA via stabilization of the overall structure of the RTBP1 DNA binding domain. When DNA bound to $RTBP1_{506-615}$, large chemical shift perturbations were induced in the N-terminal arm, helix 3, and the loop between helices 3 and 4. These results suggest that helix 3 functions as a sequence-specific recognition helix while the N-terminal arm stabilizes the DNA binding.

Telomeres, the specialized nucleoprotein complexes that physically cap and protect the chromosome ends, are essential for genome stability in all eukaryotes (*1*). The telomeric nucleoprotein complex allows cells to distinguish natural chromosome ends from double-stranded DNA breaks (*2*). Without functional telomeres, chromosome ends activate the DNA damage response pathway that induces cell cycle arrest, senescence, or apoptosis (*3*). Telomeres also protect the chromosome ends from degradation and end-to-end fusion. Eukaryotic telomeric DNA is composed of long tandem arrays of short sequence elements, such as TTAGGG in vertebrates and TTTAGGG in higher plants, followed by a single-stranded 3′-overhang (*4*). Due to the end replication problem, most dividing cells show progressive loss of telomeric DNA during successive rounds of DNA replication, eventually leading to chromosomal instability and cell death (*5*). Therefore, the extended proliferation of all eukaryotic cells requires a mechanism for counteracting the loss of telomeric DNA. In some immortalized cells, for example, telomere shortening can be avoided by activation of telomerase, the ribonucleoprotein that carries out telomere elongation (*6*).

Telomere length homeostasis is regulated by telomerase and a collection of associated proteins. Some proteins specifically bind to the single-stranded 3′-overhang at the extreme termini of chromosomes, including TEBPs from ciliated protozoa (*7*), Cdc13 from the budding yeast (*8*), Pot1 found in fungi, plants, and vertebrates (*9, 10*), and STEP1 and AtWHY1 from *Arabidopsis thaliana* (*11, 12*). These proteins have been shown to play roles in chromosome end protection and/or in telomere and telomerase regulation. Members of the other group of proteins that specifically bind

[†] This work was supported in part by grants from the Korean Ministry of Health and Welfare through the Molecular Aging Research Center, from the Korea Science and Engineering Foundation (R112000078010010 and R01-2007-000-10161-0), and from the Seoul Development Institute. This study made use of the NMR facility at the Korea Basic Science Institute, which is supported by the Bio-MR research program of the Korean Ministry of Science and Technology (E27070).

[‡] Chemical shifts of RTBP1 have been deposited in BioMagResBank (entry 11038), and coordinates of the 20 structures have been deposited in the RCSB Protein Data Bank (entry 2ROH).

* To whom correspondence should be addressed. I.K.C.: telephone, 822-2123-2660; fax, 822-364-8660; e-mail,topoviro@yonsei.ac.kr. W.L.: telephone, 822-2123-2706; fax, 822-363-2706; e-mail, wlee@spin.yonsei.ac.kr.

[§] Department of Biochemistry, Protein Network Research Center, Yonsei University.

[||] Department of Biology, Protein Network Research Center, Yonsei University.

[⊥] University of Tsukuba.

10.1021/bi801270g CCC: $40.75
Published on Web 01/16/2009

to double-stranded telomeric DNA were identified as having a DNA binding domain that is closely related to the Myb-type DNA binding motif. In humans, two homologous proteins have been identified. TRF1[1] negatively regulates telomere length by inhibiting the interaction between telomeres and telomerase (*13*), whereas TRF2, a paralog of TRF1, is required to protect chromosome ends (*14*) and stabilizes a terminal loop structure called the t-loop (*15*). The budding yeast Rap1p and the fission yeast Taz1p are proposed to be functional homologues of the human TRF proteins (*16, 17*).

Myb-containing proteins specific to double-stranded telomeric repeats have been identified in several plant species. From *Arabidopsis*, two proteins (AtTRP1 and AtTBP1) have been shown to specifically bind duplex telomeric DNA (*18, 19*). Knockouts of *AtTBP1* resulted in a deregulation of telomere length control, with elongated telomeres (*20*). In addition, at least 12 TRF-like (TRFL) proteins were shown to contain a single Myb domain (*21*). TRFL family 1 possesses a highly conserved Myb extension at the C-terminus, but TRFL family 2 proteins lack this domain. DNA binding studies with the isolated C-terminal fragments from TRFL family 1, but not family 2, showed specific binding to double-stranded telomeric repeats. In tobacco, the expression of NgTRF1 is tightly regulated in correlation with cell division and cell cycle (*22*). NgTRF1 functions as a negative regulator of telomere length (*23*). In rice, knockout plants of *RTBP1* exhibited markedly longer telomeres compared to those of wild-type plants and displayed severe developmental abnormalities in both vegetative and reproductive organs (*24*). Furthermore, inactivation of RTBP1 caused the defective phenotype with an increased frequency of anaphase bridges resulting from chromosomal fusions (*24*). These results suggest that RTBP1 is involved in the control of telomere length and telomere stability in rice plants.

Despite the apparently conserved function, one of the most striking differences between plant and mammal telomere binding proteins is the presence of a highly conserved Myb extension in plant proteins. The Myb domain of hTRF1 is sufficient for binding human telomeric DNA, but this is not the case for the plant proteins. Thus, it is of immediate interest to understand how the Myb extension contributes to DNA binding of plant telomeric proteins. The structure of the TRF1 DNA binding domain is composed of three α-helices and forms a helix−loop−helix conformation (*25*). In contrast, the structures of DNA binding domains of plant telomeric proteins such as AtTRP1 and NgTRF1 were reported to contain four α-helices (*26, 27*). Since the sequence comparison revealed that the RTBP1 DNA binding domain contains a highly homologous C-terminal Myb extension (Figure 1), we determined the three-dimensional structure of the RTBP1 DNA binding domain in solution by NMR spectroscopy. The overall structure of the RTBP1 DNA binding domain is composed of four α-helices and stabilized by three hydrophobic patches. The architecture of the first three helices in RTBP1 is similar to that in hTRF1. The additional fourth helix is essential for binding to telomeric DNA via stabilization of the overall structure of the RTBP1 DNA binding domain through hydrophobic interactions with other parts of the molecule. Thus, the Myb extension defines a novel class of telomere binding proteins in plants. In addition, we demonstrate that the RTBP1 DNA binding domain induces a DNA bending in the two-telomere repeat, suggesting a role in establishing and/or maintaining an active telomere configuration in vivo.

EXPERIMENTAL PROCEDURES

Expression and Purification of the RTBP1 Fragments. The full-length RTBP1 cDNA was amplified by polymerase chain reaction (PCR) as described previously (*28*). To obtain the deleted RTBP1 fragments, residues 506−615, 506−594, 528−615, and 528−594 of RTBP1 were PCR-amplified from pBS-RTBP1. Primers compatible with cloning into the *Bam*HI and *Sal*I restriction sites of pGEX-4T-1 (Amersham Pharmacia Biotech) were used, and the sequence of the resulting plasmids was confirmed by the dideoxy sequencing method. The GST fusion proteins were expressed in *Escherichia coli* BL21(DE3) cells via addition of 1 mM isopropyl 1-thio-β-D-galactopyranoside (IPTG), purified with glutathione-Sepharose 4B (Amersham Pharmacia Biotech), and then digested with 100 units/mL bovine thrombin (Amersham Pharmacia Biotech) to remove GST.

To generate isotopically labeled proteins for the NMR analysis, cells harboring the $RTBP1_{506-615}$ construct were grown in M9 minimal medium containing $^{15}NH_4Cl$ and/or [$^{13}C_6$]-D-glucose. The GST fusion proteins were purified with glutathione-Sepharose 4B (Amersham Pharmacia Biotech) and were then digested with 100 units/mL bovine thrombin (Amersham Pharmacia Biotech). To remove bovine thrombin, the DNA binding domain was further purified with benzamidine-Sepharose 6B (Amersham Pharmacia Biotech). The samples were then dialyzed in NMR buffer [50 mM potassium phosphate (pH 7.0), 100 mM NaCl, and 1 mM NaN_3], concentrated by the use of a centricon (Amicon) with a 5 kDa cutoff membrane, and transferred to a 5 mm symmetrical microcell (Shigemi).

Electrophoretic Mobility Shift Assay (EMSA). An electrophoretic mobility shift assay was performed with a DNA probe containing the two-telomere repeats as described previously (*28*). Briefly, the purified RTBP1 fragments were preincubated with 0.5 μg of poly(dI-dC) and 0.5 μg of nonspecific DNA oligonucleotide for 10 min on ice to reduce the level of nonspecific DNA−protein binding. End-labeled DNA probe (0.25 ng) was then added to the reaction mixtures. After being incubated for 10 min on ice, the mixtures were loaded on an 8% nondenaturing polyacrylamide gel. Binding activity was quantified with Image Gauge version 2.53 (Fuji Photofilm).

DNA Bending Assay. To generate the DNA fragments which are identical in size but differ in the location of the protein binding site, the two-telomere repeat DNA (5′-TTTAGGGTTTAGGG-3′) was inserted into DNA bending vector pBend4. To generate a series of the 139 bp permuted DNA probes, the resulting plasmid was digested with restriction enzymes (*Mlu*I, *Bgl*II, *Spe*I, *Xho*I, *Eco*RV, *Pvu*II,

[1] Abbreviations: TRF1, telomeric repeat binding factor 1; RTBP1, rice telomere binding protein 1; AtTRP1, *Arabidopsis thaliana* telomere binding protein 1; AtTBP1, *A. thaliana* telomeric repeat binding protein 1; NgTRF1, *Nicotiana glutinosa* telomeric repeat binding factor 1; TRFH, TRF homology domain; HTH, helix−turn−helix; GST, glutathione *S*-transferase; NMR, nuclear magnetic resonance; ITC, isothermal titration calorimetry; rmsd, root-mean-square deviation; NOE, nuclear Overhauser effect; NOESY, nuclear Overhauser effect spectroscopy; TOCSY, total correlated spectroscopy; HSQC, heteronuclear single-quantum coherence.

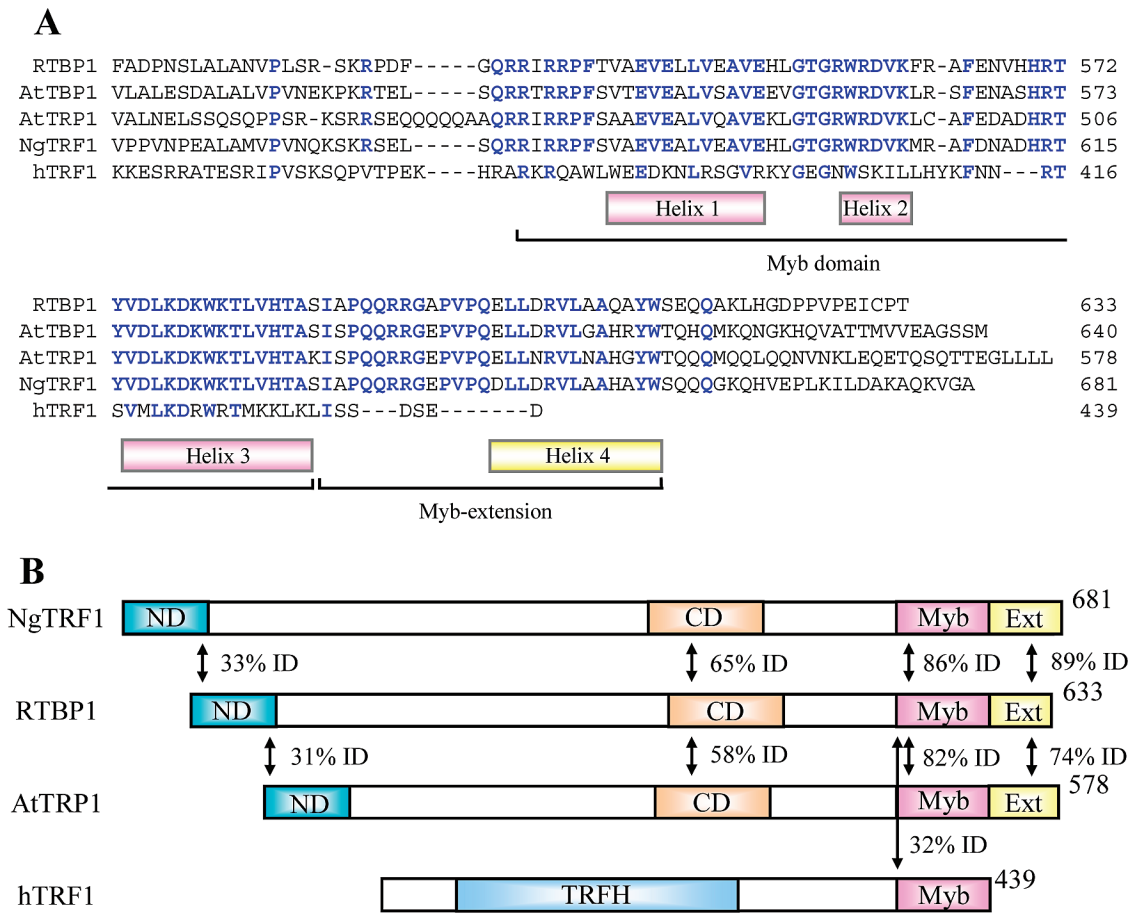

FIGURE 1: Comparison of the RTBP1 DNA binding domain with the corresponding regions of other telomere binding proteins. (A) Sequence alignment of the DNA binding domains of RTBP1 (rice), AtTBP1 (*A. thaliana*), AtTRP1 (*A. thaliana*), NgTRF1 (tobacco), and hTRF1 (human). Amino acid residues in RTBP1 that are identical to those of the other proteins are colored blue. The positions of the four helices constituting the DNA binding domain are indicated below the sequence. (B) Comparison of the domain structures of RTBP1 with NgTRF1, AtTRP1, and hTRF1. The percentage of amino acid identity is indicated. Myb, Myb domain; Ext, Myb extension domain; ND, N-terminal domain; CD, central domain; TRFH, TRF homology domain; ID, amino acid identity.

*Sma*I, *Kpn*I, and *Bam*HI), and the products were end-labeled with [γ-^{32}P]ATP and T4 polynucleotide kinase. The EMSA was carried out as described above, and the migration of the complexes was analyzed as described previously (*29*).

Isothermal Titration Calorimetry. ITC experiments were performed using a VP-ITC system (MicroCal) at 25 °C in NMR buffer. In each titration, 70 μM RTBP1$_{506-615}$ in the cell was titrated with 40 injections of 400 μM DNA. The volume of each injection was 6 μL, and injections were continued beyond saturation levels to allow for the determination of the heat of DNA dilution. The resulting data were fit to a two-site binding isotherm after subtraction of the heat of dilution, using Microcal Origin for the ITC data analysis.

Size Exclusion Chromatography. Size exclusion chromatography was performed using Superdex 75 (GE Health care) in an ACTA prime system (Amersham Biotech). RTBP1$_{506-615}$ and the RTBP1$_{506-615}$−DNA complex in NMR buffer were loaded on a column at 25 °C. The elution profile was monitored by absorbance of 280 nm. On the basis of the saturation point which was determined by ITC experiments, the saturated complex sample was prepared and loaded on the column. Molecular mass markers (Sigma) containing albumin (66 kDa), carbonic anhydrase (29 kDa), cytochrome *c* (12.4 kDa), and aprotinin (6.5 kDa) were used to obtain a standard curve.

NMR Spectroscopy. NMR experiments were performed in a solvent mixture of 90% $^{1}H_2O$ and 10% $^{2}H_2O$ or 99.9% $^{2}H_2O$ in NMR buffer using a Bruker DRX 500 MHz or 900 MHz instrument equipped with a Cryo-probe system at 303 K. ^{1}H chemical shifts were referenced directly to internal 4,4-dimethyl-4-silapentane-1-sulfonic acid (DSS) in solvent. ^{15}N and ^{13}C chemical shifts were referenced indirectly. All spectra were processed using XWIN-NMR (Bruker Biospin Corp.) and NMRPipe/NMRDraw and analyzed using Sparky 3.60. The two-dimensional (2D) ^{1}H−^{15}N HSQC (*30*), constant time ^{1}H−^{13}C HSQC (*31*), three-dimensional (3D) HNCA, HN(CO)CA, HNCO, HNCACB, and CBCA(CO)NH (*32*, *33*) experiments were performed for the backbone assignments. Highly overlapped peaks were resolved using 3D HNCO. Proton assignments were executed using 3D HNHA (*34*), HBHANH (*35*), ^{15}N-edited TOCSY-HSQC (*36*), and HCCH-TOCSY (*37*). Carbon chemical shifts were obtained by HNCA, HNCACB, CBCA(CO)NH, and HNCO and CC(CO)NH (*35*).

To obtain the NOEs, ^{15}N-edited NOESY and ^{13}C-edited NOESY experiments (*38*) were performed in a mixture of 90% H_2O and 10% $^{2}H_2O$ with a mixing time of 100−150 ms at 303 K. ^{13}C-edited NOESY experiments were also conducted in 99.9% $^{2}H_2O$ in NMR buffer. The sequential assignments were determined by NOEs [$d_{NN(i,i+1)}$ and $d_{\alpha N(i,i+1)}$] from ^{15}N-edited NOESY. The side chain assign-

ments were completed by HCCH-TOCSY and ^{13}C-edited NOESY experiments conducted in a 99.9% ^2H_2O solution. The angle constraints were obtained from 3D HNHA experiments and TALOS. The hydrogen bond constraints were collected from H−D exchange experiments. To identify slowly exchanging amide protons, the purified proteins were lyophilized and dissolved in 99% ^2H_2O in NMR buffer. Two-dimensional (2D) ^{1}H−^{15}N HSQC spectra were recorded immediately or in a day.

For analysis of the RTBP1−DNA complex, 2D ^{1}H−^{15}N TROSY-HSQC (*39*) and proton one-dimensional (1D) NMR experiments were performed using a Bruker DMX 500 MHz instrument at 303 K. The hydrogen bond signals of DNA (12−14 ppm) and backbone ^{1}H−^{15}N correlation signals of RTBP1 were obtained by a 1D ^{1}H NMR experiment and a 2D ^{1}H−^{15}N TROSY-HSQC experiment, respectively. The titration experiments were conducted at various molar ratios of RTBP1 with respect to DNA concentration.

Structure Calculation. Structure calculations were performed using CYANA version 2.1 (*40*). Distance restraints were derived from ^{15}N-edited NOESY and ^{13}C-edited NOESY with mixing times of 100 and 150 ms, respectively. Chemical shift tolerances for automatic NOE assignments were set at 0.030 or 0.035 ppm for protons, 0.25 ppm for carbons, and 0.4 ppm for nitrogens. NMR-derived experimental restraints contained 1379 unambiguous NOEs [836 short-range NOEs ($|i - j| \leq 1$), 331 medium-range NOEs ($1 < |i - j| < 5$), and 212 long-range NOEs ($5 \leq |i - j|$)], 94 torsion angle restraints, and 64 hydrogen bonding restraints, which were used for the structure calculation. A total of seven cycles of CYANA calculation were executed in 16 nodes of a Linux cluster computer. Twenty structures with the lowest energy were analyzed using PROCHECK and displayed using PyMOL (DeLano Scientific LLC) with APBS and MOLMOL.

RESULTS

Identification of the Minimal DNA Binding Domain of RTBP1. A sequence alignment of the Myb-containing regions of plant telomere binding proteins with the corresponding region in hTRF1 revealed a plant-specific Myb extension region C-terminal to the Myb domain (Figure 1). Both the Myb domain and the Myb extension domain have been shown to be required for binding to plant telomeric DNA (*20, 26, 27*). Closer inspection of the entire sequence comparison showed that the DNA binding domain of RTBP1 displays a high degree of sequence identity with other plant proteins (Figure 1B). Two additional regions, including the N-terminal domain (ND) and the central domain (CD), exhibit substantial sequence conservation among plant telomere binding proteins. However, these regions exhibit no sequence homology with the TRFH domain in hTRF1 and are absent in vertebrate TRF proteins (Figure 1B).

We have previously identified the C-terminal 110-amino acid region (residues 506−615) as the structured telomere binding domain in RTBP1 (*28*). To determine the minimal domain of RTBP1 for specific binding to plant telomeric DNA, the purified GST fusion proteins (RTBP1$_{506-615}$, RTBP1$_{506-594}$, RTBP1$_{528-615}$, and RTBP1$_{528-594}$) were digested with thrombin to remove GST (Figure 2A,B) and used in the electrophoretic mobility shift assay with the two-

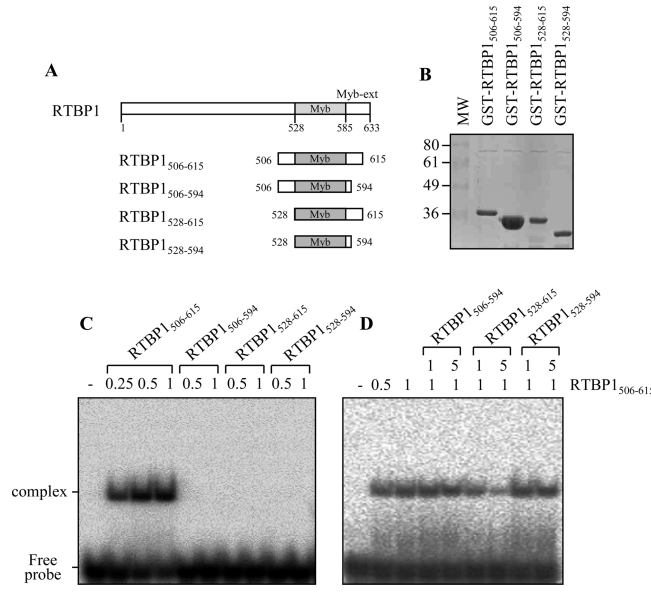

FIGURE 2: Identification of the minimal DNA binding domain of RTBP1. (A) Schematic representation of the four RTBP1 fragments (RTBP1$_{506-615}$, RTBP1$_{506-594}$, RTBP1$_{528-615}$, and RTBP1$_{528-594}$) that differ in size. The RTBP1 fragments were fused to GST and used in the electrophoretic mobility shift assay. (B) Recombinant GST fusion proteins were purified on glutathione-Sepharose 4B, separated via SDS−PAGE, and stained with Coomassie Blue. (C) Electrophoretic mobility shift assay performed with the labeled probe containing the two-telomere repeat sequence and recombinant proteins at concentrations of 0.25, 0.5, and 1 μM as indicated. The complexes were resolved on an 8% nondenaturing polyacrylamide gel, and the positions of the complex and free probe are shown. (D) Two different length proteins were mixed in different molar ratios before the addition of DNA probe as indicated.

telomere repeat sequence. RTBP1$_{506-615}$ gave rise to a discrete DNA−protein complex that migrated more slowly than the free probe (Figure 2C). However, deletion of 21 residues from the C-terminus of RTBP1$_{506-615}$ completely abolished the telomere binding activity, indicating that Myb extension spanning residues 595−615 is required for binding to plant telomeric DNA. Notably, deletion of 22 residues from the N-terminus of RTBP1$_{506-615}$ also abolished the binding activity, although fragment RTBP1$_{528-615}$ contains both the Myb domain and the Myb extension. These results indicate that RTBP1, unlike AtTRP1, requires in addition residues 506−527 at the N-terminus of the Myb domain for telomere binding. No shifting complex was detected in the assay with RTBP1$_{528-594}$ that includes only the Myb domain.

Although full-length hTRF1 binds to telomeric DNA as a preformed homodimer in vivo, the isolated Myb domain of hTRF1 is capable of sequence-specific binding as a monomer in vitro (*41*). We have previously demonstrated that two molecules of RTBP1$_{506-615}$ can bind to the two-telomere repeat sequence (*28*). To examine whether two RTBP1 proteins bind telomeric repeat separately or as a dimer, we performed the electrophoretic mobility shift assay using the mixtures of RTBP1$_{506-615}$ and the truncated fragments. As shown in Figure 2D, the intensity of shifting bands detected in RTBP1$_{506-615}$ did not decrease upon the addition of increasing amounts of RTBP$_{506-594}$ or RTBP1$_{528-594}$. In contrast, the signal was slightly diminished in the presence of the same molar excess of RTBP1$_{528-615}$ and significantly reduced with a 5-fold excess, indicating that addition of RTBP1$_{528-615}$, which itself cannot bind DNA, attenuates the

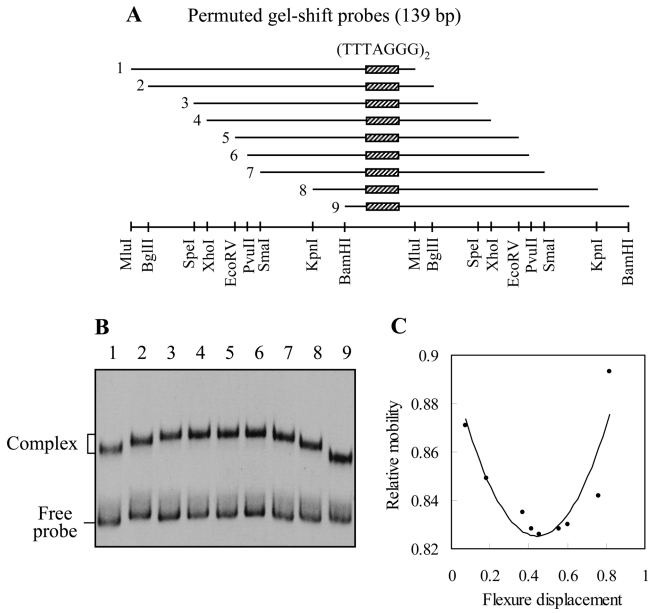

FIGURE 3: DNA bending induced by $RTBP1_{506-615}$ binding to telomeric DNA. (A) Schematic representation of nine permuted mobility shift probes carrying the two-telomere repeats. (B) Electrophoretic mobility shift assay performed with $RTBP1_{506-615}$ and the permuted probes. The positions of the complex and free probe are shown. (C) Relative mobility (mobility of complex/mobility of free probe) of the protein−DNA complex plotted against the flexure displacement in each probe. The data points represent probes 1−9 from right to left. The values on the *x*-axis indicate the distance from the middle of the telomeric repeat site to the 5′-end of the probe divided by the length of the probe.

binding of $RTBP1_{506-615}$ to DNA. Furthermore, the mixture of $RTBP1_{506-615}$ and $RTBP1_{528-615}$ was found to form a single complex that comigrated with the $RTBP1_{506-615}$ complex. These results suggest that the protein−protein interactions through the Myb extension (residues 594−615) may be involved in binding of RTBP1 to telomeric DNA.

RTBP1 Bends Telomeric DNA. Some Myb-containing proteins such as hTRF1, yeast Rap1, and AtTBPs have been shown to induce a bend in the telomeric repeat sequences (*42*). To determine whether RTBP1 displays this feature, we employed the circular permutation assay. The telomeric DNA was inserted into pBend4 and digested with various restriction enzymes to produce nine DNA fragments of equal length, each harboring a RTBP1 binding site at a different position relative to the ends of the molecules (Figure 3A). Because the isolated RTBP1 DNA binding domain formed a single complex with two copies of the TTTAGGG repeat (*28*), the permuted probes, which carried the two-telomere repeats, were generated. DNA probes were incubated with purified $RTBP1_{506-615}$, and the mobility of the resulting protein−DNA complexes was analyzed on nondenaturing polyacrylamide gels. The position of the RTBP1 binding site in permuted DNA probes had an effect on migration of the complexes. As the binding site for RTBP1 was located more centrally in the probes, the complexes migrated more slowly, indicating that DNA bending was induced on the two-telomere repeats upon RTBP1 binding (Figure 3B). We observed a slight difference in the mobility of the free probes, suggesting an intrinsic curvature of the two-telomere repeat.

To estimate the extent of DNA bending induced by $RTBP1_{506-615}$ binding, the relative mobility of each complex was plotted against the flexure displacement, and the data points were interpolated with a quadratic function to deduce a value of the deviation from linearity (Figure 3C). The degree of DNA bending was calculated to range from 38° to 41° in three independent experiments, indicating that $RTBP1_{506-615}$ induced a shallow DNA distortion in which the DNA deviates from linearity by ~40°. A similar angle of DNA bend was found in accordance with the equation derived by Thompson and Landy (*29*).

Three-Dimensional Structure of $RTBP1_{506-615}$ in Solution. To investigate the molecular interactions between the RTBP1 DNA binding domain and telomeric DNA at atomic-level resolution, we determined the three-dimensional structure of $RTBP1_{506-615}$ in solution by NMR spectroscopy. Complete NMR resonance assignments were executed using conventional backbone experiments and side chain experiments in a Bruker DRX 500 MHz or 900 MHz instrument equipped with a Cryo-probe system (*43*). As shown in Figure 4, the NOE bar diagram clearly indicates that the DNA binding domain of RTBP1 contains four helical regions and three connecting loops as found in other plant telomere binding proteins (*26, 27*). These results were confirmed by TALOS analysis and a H−D exchange experiment. Structural statistics for the DNA binding domain of RTBP1 are summarized in Table 1. An ensemble of 20 energy-minimized structures and a ribbon diagram are shown in panels A and B of Figure 5, respectively. The N-terminal region was not able to converge due to intrinsic flexibility. Solution structures of $RTBP1_{506-615}$ were well defined with a root-mean-square deviation (rmsd) of 0.75 ± 0.14 Å for the backbone atoms except the N-terminal region (residues 506−535). When secondary structural regions were superimposed, the rmsd was 0.35 ± 0.15 Å for the backbone atoms. Although the helix regions were well-defined, the loop regions showed some variations. Loop 1 (residues 554−559) exhibited flexible structure due to a lack of NOEs that were commonly observed in solution structures of other telomere binding proteins (*25*−*27*), and loop 2 (residues 565−572) also exhibited its flexibility. Helix 1 (residues 538−553), helix 2 (residues 560−564), and helix 3 (residues 573−586) are located in the Myb domain of RTBP1. Loop 3 (residues 587−600) and helix 4 (residues 601−614) comprised the C-terminal Myb extension domain which is a unique feature of plant double-stranded telomere binding proteins.

The overall structure of $RTBP1_{506-615}$ is mostly stabilized by three hydrophobic patches composed of interactions among residues in the helices (Figure 5C). The residues involved in the formation of the hydrophobic patches are highly conserved in other Myb-containing proteins (Table 2). Leu576 in helix 3 interacts with Ala548 in helix 1 and Val560 in helix 2 to form hydrophobic patch 1 (Figure 5D). These hydrophobic interactions play a major role in stabilizing the overall topology of the three helices located in the Myb domain. In the three-helix bundle of the Myb domain, the second and third helices exhibited a typical helix−turn−helix (HTH) motif for binding telomeric DNA. This mode of DNA interaction is similar to those found in other telomere binding proteins (*25*). Trp580, Leu583, and Val584 at the end of helix 3 interacted with Leu545, Val546, and Val549 from helix 1 and Val607 form helix 4 to form hydrophobic patch 2 (Figure 5E). This hydrophobic patch contributes to the proper packing of helices 1, 3, and 4. In addition, hydrophobic patch 3 was formed by hydrophobic interactions between Val539

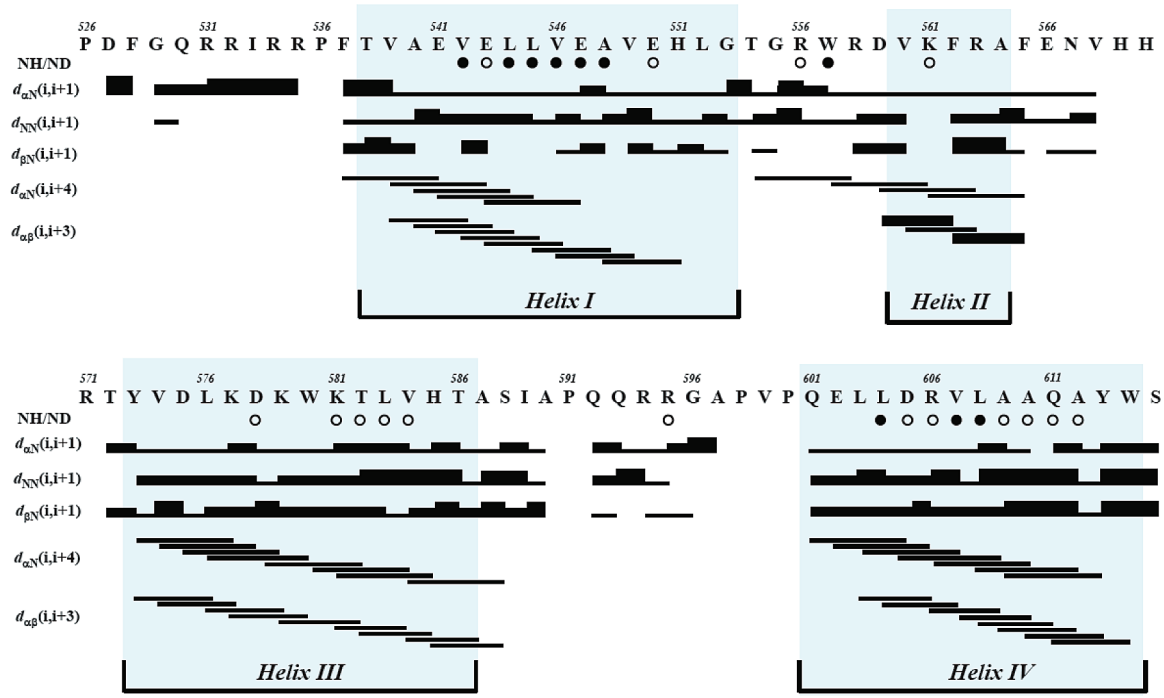

FIGURE 4: Secondary structure elements and a summary of NOE connectivity of $RTBP1_{506-615}$. The NOE connectivities were summarized by the line thickness classified by NOE intensity. NOEs were extracted from ^{15}N-edited NOESY and ^{13}C-edited NOESY spectra. Slowly exchanging residues that remained for more than 1 day are denoted with filled circles, and those that disappeared in 10 min are denoted with empty circles. The amino acid sequence for $RTBP1_{506-615}$ is shown, and the helical regions are denoted with gray boxes.

Table 1: Structural Statistics for the DNA Binding Domain of RTBP1

no. of distance restraints	
all	1379
intraresidue	406
sequential ($\|i - j\| = 1$)	430
medium-range ($2 \leq \|i - j\| \leq 5$)	331
long-range ($\|i - j\| > 5$)	212
no. of hydrogen bond restraints[a]	64
no. of dihedral angle restraints	
all	94
Φ	47
Ψ	47
mean CYANA target function ($Å^2$)[b]	2.37 ± 1.01
rmsd from the average coordinate (Å)	
backbone atoms	0.75 ± 0.14
residues 536−615, helix region only	0.35 ± 0.15
heavy atoms of residues 536−615	1.55 ± 0.16
Ramachandran analysis (%)	
residues in most favored regions	77.0
residues in additional allowed regions	22.3
residues in generously allowed regions	0.6
residues in disallowed allowed regions	0

[a] Two restraints for each hydrogen bond. [b] No distance and angle restraint violations are observed during structure refinement.

and Val542 in helix 1 and Leu603 in helix 4 (Figure 5F). These interactions stabilize the architecture of helices 1 and 4. In the overall shape of $RTBP1_{506-615}$, helix 3 is perpendicular to the axes of helices 1, 2, and 4, and helix 4 orients nearly parallel to helix 1.

Structural Comparison of $RTBP1_{506-615}$ with the DNA Binding Domains of Other Telomeric Proteins. A structural comparison showed that the backbone architecture of the first three helices of $RTBP1_{506-615}$ is close to that of the hTRF1 DNA binding domain (Figure 6A). The rms difference of the backbone atoms between $RTBP1_{506-615}$ and the TRF1 DNA binding domain is 2.517 Å, suggesting that two proteins may bind DNA in a similar way. This structural similarity is consistent with conservation of the hydrophobic residues in the Myb domain involved in the formation of the hydrophobic core (Table 2). However, helix 3 of the RTBP1 DNA binding domain is slightly longer than the corresponding helix of hTRF1. The hydrophobic residues (Trp580, Leu583, and Val584) at the C-terminal end of the longer helix 3 interact with helices 1 and 4 to support the overall architecture of the RTBP1 DNA binding domain.

Superimposition of the solution structures of $RTBP1_{506-615}$ and $NgTRF1_{561-681}$ revealed that the two structures adopt a similar fold with a rmsd of 2.027 Å for the backbone atoms (Figure 6B). In contrast, despite a tremendous sequence identity, the structure of the DNA binding domain of RTBP1 is different from that of AtTRP1 reported previously (*26*) (Figure 6C). The rms difference between the backbone atoms of the RTBP1 DNA binding domain and the corresponding atoms of AtTRP1 is 7.271 Å. Even when the structural comparison was restricted to the first three helices, the rms difference was 4.832 Å for the backbone atoms. While helices 1 and 2 in AtTRP1 orient roughly parallel with each other, helix 1 in RTBP1 orients nearly parallel to helix 4.

Binding of $RTBP1_{506-615}$ to Telomeric DNA. To examine the telomeric DNA binding mode of $RTBP1_{506-615}$, we performed the titration experiments using 1D NMR spectroscopy with the two-telomere repeat sequence. The analysis was carried out by NMR after a change in the chemical shifts of the imino proton signals on double-stranded telomeric DNA. The original free-form resonances of the imino protons of DNA are gradually changed as increasing concentrations of protein are added (Figure 7A). After a molar ratio of 2:1 RTBP1 to DNA was reached, the imino proton chemical shifts remained unchanged.

We next performed a series of isothermal titration calorimetry (ITC) experiments to assess the binding of $RTBP1_{506-615}$ to telomeric DNA under the same conditions in

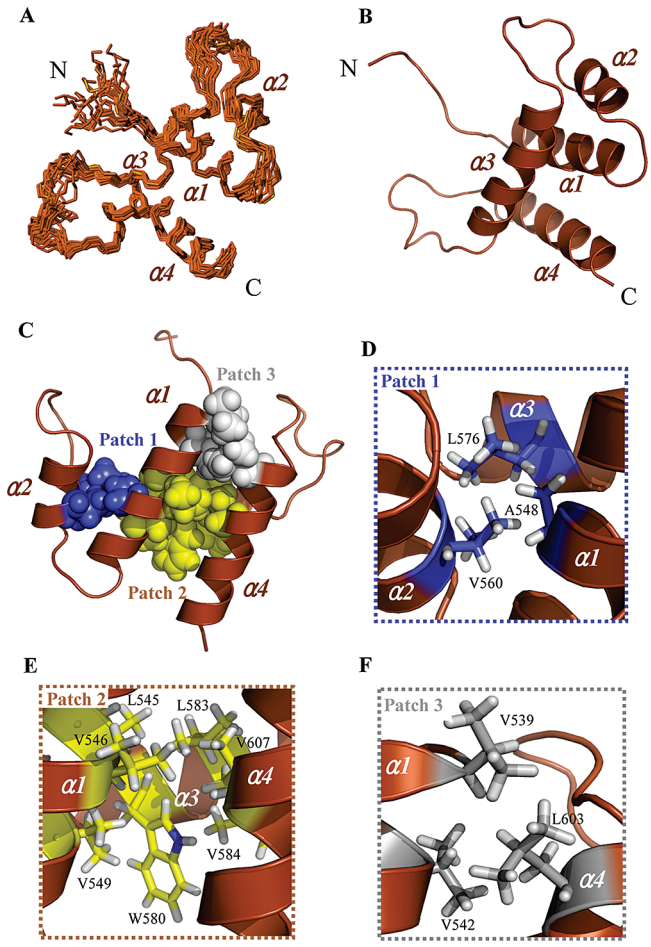

FIGURE 5: Solution structure of RTBP1$_{506-615}$. (A) Backbone superposition of 20 energy-minimized structures of the RTBP1 DNA binding domain. The Myb-type domain consists of the first three helices, and the C-terminal Myb extension domain contains the fourth helix. The helices are numbered in sequence from the N- to C-terminus. (B) Overall structure of RTBP1$_{531-615}$ in ribbon representation. (C) Three hydrophobic patches that contribute to stabilizing the overall architecture of the protein. (D) Patch 1 (colored blue) stabilizes the overall folding of the first three helices. (E) Patch 2 (colored yellow) maintains the proper orientation of helices 1, 3, and 4. (F) Patch 3 (colored gray) stabilizes the architecture of helices 1 and 4.

which the NMR experiments were carried out. The integrated binding isotherms were fitted to a two-site binding model. This binding model implies that the two-telomere repeat sequence presents two binding sites for RTBP1$_{506-615}$. The ITC isotherm shown in Figure 7B provides evidence for protein−protein interactions which appear as weak positive cooperativity. The qualitative evidence for this is the slight increase in the enthalpy of binding for the initial injections. For completely independent sites, this portion of the isotherm would be flat. Thus, the ITC analysis indicates that two molecules of RTBP1$_{506-615}$ interact with telomeric DNA cooperatively at a molar ratio of 2:1 (protein:DNA). These results are consistent with the data in Figure 2D showing the weak protein−protein interactions between RTBP1$_{506-615}$ and the non-DNA binding RTBP1$_{528-615}$.

To further confirm that two molecules of the RTBP1 DNA binding domain bind to the two-telomere repeat sequence, we performed size exclusion chromatography (Figure 7C). RTBP1$_{506-615}$ elutes on a Superdex 75 column as a single peak with an apparent molecular mass of 14.1 kDa that is close to the predicted mass of monomeric RTBP1$_{506-615}$ (12.1 kDa). Longer incubation of RTBP1$_{506-615}$ shows no change in the elution pattern (data not shown). On the basis of the saturation point which was determined by ITC experiments, RTBP1$_{506-615}$ and the two-telomere repeat were mixed and loaded on the column. RTBP1$_{506-615}$ complexed with DNA exists as a single peak with an apparent molecular mass of 33.4 kDa. On the basis of the molecular masses of 12.1 kDa for RTBP1$_{506-615}$ and 8.5 kDa for telomeric DNA, it is estimated that two molecules of RTBP1$_{506-615}$ are present in a single protein−DNA complex. SDS−PAGE and agarose gel electrophoresis were used to show contents of the peaks (Figure 7D).

Specific Residues in RTBP1$_{506-615}$ Interact with Telomeric DNA. To identify specific residues that interact with telomeric DNA, we analyzed the chemical shift changes in the 2D HSQC spectra upon interaction of RTBP1$_{506-615}$ with telomeric DNA. Since two molecules of RTBP1$_{506-615}$ can bind to telomeric DNA, the characteristic resonances observed in the DNA-free RTBP1 were completely shifted to the DNA-bound positions at an RTBP1:DNA molar ratio of 2.5:1. The majority of residues that exhibited large chemical shift perturbations ($\Delta\delta$ > 0.3 ppm) are located in the N-terminal arm, helix 3, and the loop between helices 3 and 4 (Figure 8A,B). The residues that did not show large chemical shift changes upon DNA binding are primarily located on the α-helix regions except helix 3, suggesting that the chemical shift changes may not result from global structural changes but are due to the DNA binding interaction. Notably, the resonance peaks of three residues (marked with a brown asterisk in Figure 8A) in the N-terminal region (Ser523, Lys524, and Phe528) disappeared due to extensive line broadening upon addition of two repeats of telomeric DNA. This observation is consistent with the electrophoretic mobility shift data showing that the 22 N-terminal residues are required for telomeric DNA binding.

In both hTRF1 and NgTRF1, helix 3 functions as a DNA recognition helix to interact with the major groove of the DNA whereas the short N-terminal arm interacts with the minor groove of the DNA (*25, 27*). Consistent with these previous reports, the residues of the RTBP1 DNA binding domain that are involved in DNA recognition are conserved in hTRF1 and NgTRF1 (Table 3). These results suggest that RTBP1 could bind DNA in a similar architecture with hTRF1 and NgTRF1. Importantly, the perturbed residues in helix 3 (Lys577, Lys581, and His585) upon DNA binding are located on one side of the α-helix, enabling DNA binding. The residues of the loop between helices 3 and 4 in RTBP1 (Ser588, Ala590, Gln592, and Gly596) exhibited significant chemical shift perturbations, indicating that the Myb extension could be involved in DNA recognition.

The RTBP1 DNA binding domain has a characteristic electrostatic surface that contributes to specific interaction with telomeric DNA (Figure 8C). The majority of the residues that showed significant chemical shift perturbations are distributed on the positively charged surface around the HTH motif and at the N-terminal arm. In contrast, most of the hydrophobic residues that did not interact with DNA are distributed on the reverse side against the HTH motif. The chemical shift perturbation data match well the surface charge distribution plot, suggesting that positive surface of the

Table 2: Structural Comparison of $RTBP1_{506-615}$ and the DNA Binding Domains of Other Telomere Binding Proteins

	$RTBP1_{506-615}$	$NgTRF1_{561-681}$	$AtTRP1_{464-560}$	$hTRF1_{378-439}$	secondary structure[a]
rmsd[b]	–	2.027 Å	7.271 Å	2.517 Å	
hydrophobic patch 1	Ala548	Ala591	–	–	helix1
	Val560	Val603	Val494	Ile406	helix2
	Leu576	–	Leu510	Leu420	helix3
hydrophobic patch 2	Leu545	Leu588	Leu479	Leu391	helix1
	Val546	Val589	Val480	–	helix1
	Val549	Val592	Val483	Val395	helix1
	Trp580	Trp623	Trp514	Trp424	helix3
	Leu583	Leu626	Leu517	Met427	helix3
	Val584	Val627	Val518	–	helix3
	Val607	Val650	Val541	–	helix4
hydrophobic patch 3	Val539	Val589	–	–	helix1
	Val542	Val592	–	–	helix1
	Leu603	Leu646	Leu537	–	helix4
	–	–	Aal544	–	helix4
	–	–	Trp548	–	helix4

[a] Secondary structure denotes the α-helix containing the indicated residues. [b] rmsd is the structural difference for the backbone atoms between $RTBP1_{506-615}$ and the DNA binding domains of other telomeric proteins.

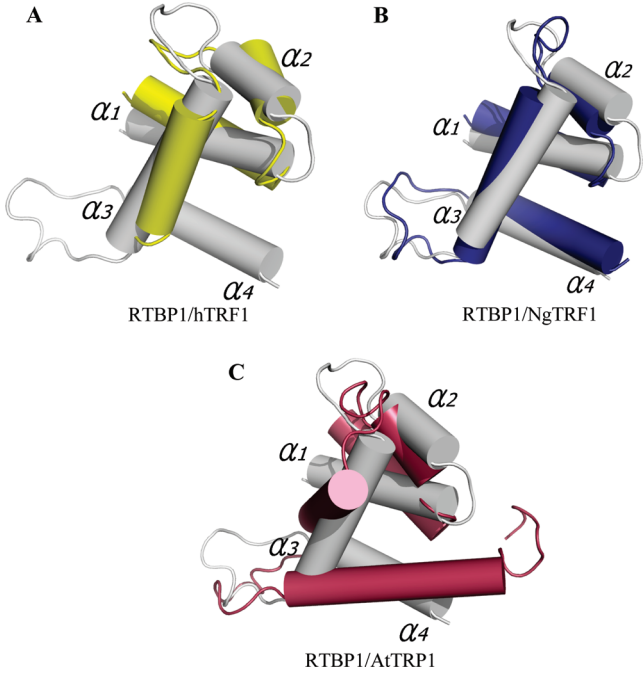

FIGURE 6: Structural comparison of $RTBP1_{506-615}$ with the DNA binding domains of other telomere binding proteins. (A) Superposition of $RTBP1_{506-615}$ (colored gray) and the hTRF1 DNA binding domain (colored yellow). (B) Superposition of $RTBP1_{506-615}$ and the NgTRF1 DNA binding domain (colored blue). (C) Superposition of $RTBP1_{506-615}$ and the AtTRP1 DNA binding domain (colored violet).

RTBP1 DNA binding domain could be involved in sequence-specific DNA recognition.

DISCUSSION

Plant proteins that specifically bind to double-stranded telomeric DNA are similar in structure to vertebrate TRFs as they carry a Myb-related DNA binding domain. A sequence alignment of the Myb-containing region of plant telomere-binding proteins with the corresponding region in hTRF1 revealed a plant-specific Myb extension domain at the C-terminal end. Although the Myb-type DNA binding domain is common in all telomere-binding proteins, the C-terminal Myb extension is absent in hTRF1 which terminates immediately adjacent to the Myb domain. In addition to the three helical regions found in the Myb domain, the fourth helix has been shown to be essential for DNA recognition in plant telomere binding proteins (*26, 27*). Thus, the Myb extension is a unique feature found in plant telomere binding proteins.

Two juxtaposed Myb domains are required for the sequence-specific recognition of telomere binding proteins (*25, 44*). The DNA binding domain of c-Myb consists of three imperfect tandem repeats (*45*). For the sequence-specific DNA binding of c-Myb, the second and third repeats are closely packed in the major groove of DNA. Although the isolated Myb domain of hTRF1 binds specifically and with a significant affinity to telomeric DNA as a monomer (*41*), hTRF1 forms a stable homodimer with its central TRFH domain and binds to telomeric repeats through its C-terminal Myb domain (*42*). Full-length dimeric hTRF1 binds to telomeric DNA by engaging two Myb domains on DNA. Like hTRF1, plant telomere binding proteins contain only a single Myb domain in their C-terminus, but there is no known dimerization domain in RTBP1. Our data from 1D NMR titration and size exclusion chromatography support the conclusion that two molecules of the RTBP1 DNA binding domain can bind to the two-telomere repeat sequence. However, it is not clear whether two RTBP1 proteins bind telomeric DNA separately or as a dimer. $NgTRF1_{561-681}$ also has been shown to bind two repeats of telomeric DNA at a molar ratio of 2:1 (protein:DNA) with high affinity (*27*). However, as manifested in the crystal structure of $NgTRF1_{561-681}$ and the telomeric DNA complex, each molecule can bind telomeric DNA as a monomer. On the basis of amino acid sequence and structural similarities of $RTBP1_{506-615}$ and $NgTRF1_{561-681}$, two RTBP1 proteins appear to bind telomeric DNA separately. Moreover, we found that $RTBP1_{506-615}$ exists as a monomer under the conditions for the NMR experiments. This was further confirmed by size exclusion chromatography.

However, the electrophoretic mobility shift data in Figure 2D show that addition of $RTBP1_{528-615}$, which itself cannot bind DNA, attenuates the binding of $RTBP1_{506-615}$ to DNA. This suggests that protein−protein interactions between two RTBP1 molecules may play a role in its binding to telomeric DNA. Furthermore, The ITC analysis provides evidence for protein−protein interactions which appear as weak positive

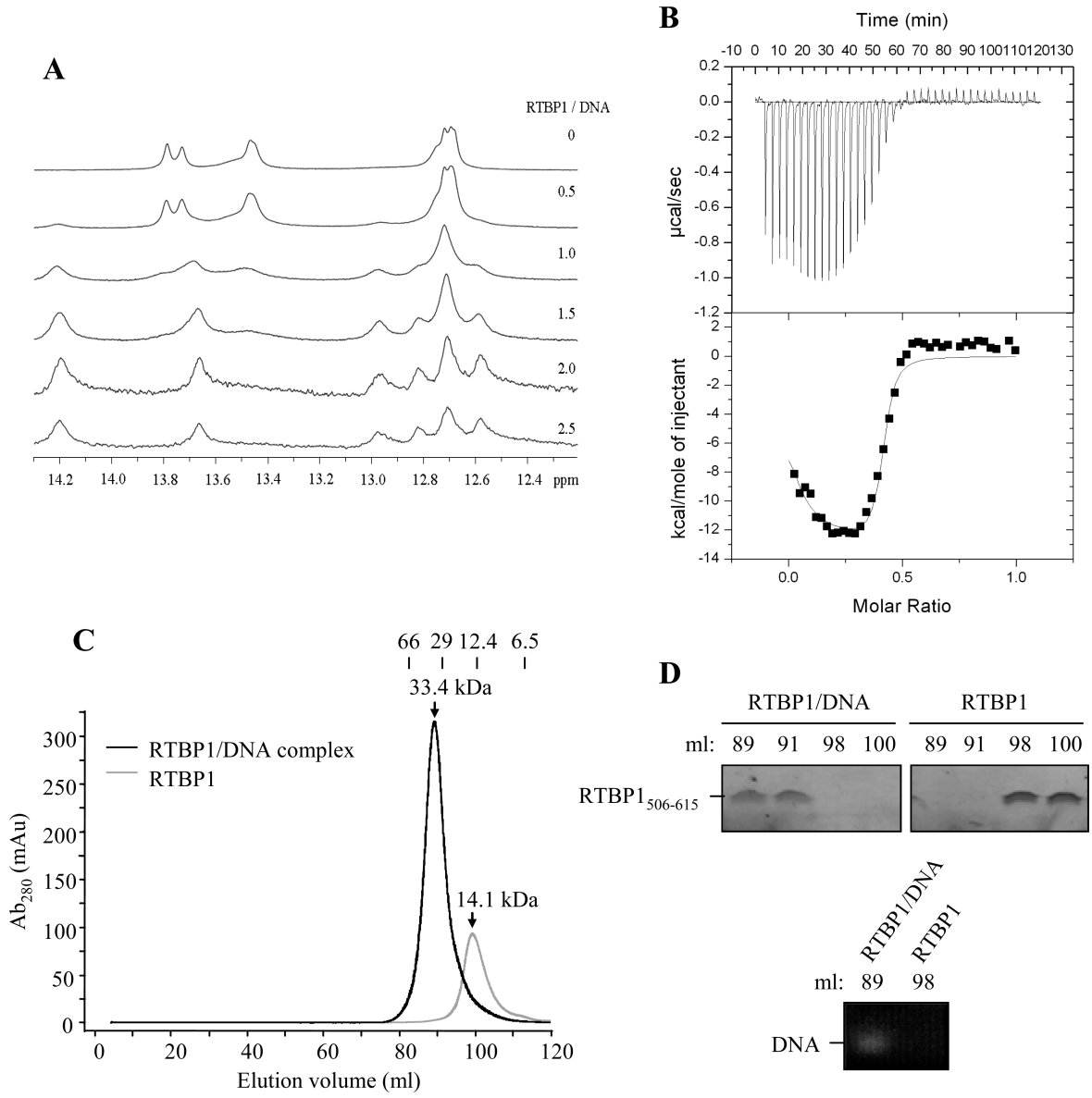

FIGURE 7: Charaterization of $RTBP1_{506-615}$ binding to telomeric DNA. (A) Titration experiments of $RTBP1_{506-615}$ with the two-telomere repeat sequence. The chemical shift changes of hydrogen bond signals of DNA were observed at the indicated protein:DNA molar ratios. (B) Representative isothermal titration of telomeric DNA with $RTBP1_{506-615}$. Telomeric DNA (400 μM) was injected into the sample cell containing 70 μM $RTBP1_{506-615}$. The top panel shows the observed heats of binding for the 2nd through 40th injections of 6 μL of DNA solution into protein after baseline subtraction. The bottom panel shows a nonlinear least-squares fit of the data varying the stoichiometry (n), the enthalpy of the reaction (ΔH), and the association constant (K_a). (C) Size exclusion chromatography of the RTBP1 DNA binding domain and the RTBP1−DNA complex. The elution profiles of $RTBP1_{506-615}$ and the $RTBP1_{506-615}$−DNA complex are shown as gray and black lines, respectively. Molecular masses (kilodaltons) of marker proteins are shown above. (D) SDS−PAGE and agarose gel electrophoresis were used to show protein and DNA contents of the peaks, respectively.

cooperativity. Telomeres are composed of a tandem array of simple repeat sequences containing a number of closely spaced binding sites. The two molecules can interact with the closely spaced telomeric repeats with no steric hindrance, since adjacent domains are bound on opposite faces of the DNA double helix (*27, 41*). Recognition of telomeric DNA by two molecules may provide a means increasing DNA binding affinity and specificity. Thus, it is reasonable to propose that protein−protein interactions through the Myb extension may facilitate the cooperative binding by RTBP1. By itself, monomeric RTBP1 may have a low affinity for a single binding site on telomeric repeats. Protein−protein interactions between two RTBP1 molecules may add to the overall stability of the protein−DNA complex, so that the two domains bind to telomeric repeat sequences cooperatively. Consistent with this hypothesis, TRFL family 1 proteins form *Arabidopsis* have been shown to form both homodimers and heterodimers via the Myb extension domains in vitro (*21*).

One of the most striking differences between RTBP1 and hTRF1 is the presence of a plant-specific Myb extension at the C-terminus. Deletion of helix 4 completely abolished the DNA binding capacity of $RTBP1_{506-615}$. The presence of the unique fourth helix appears to be essential for maintaining the structural integrity and for aiding in the DNA binding affinity and specificity. Recently, we have reported that the loop between helix 3 and helix 4 in NgTRF1 interacts with the minor groove of DNA, while the HTH motif binds to the major groove of DNA (*27*). On the basis of the structural similarity between RTBP1 and NgTRF1, the Myb extension

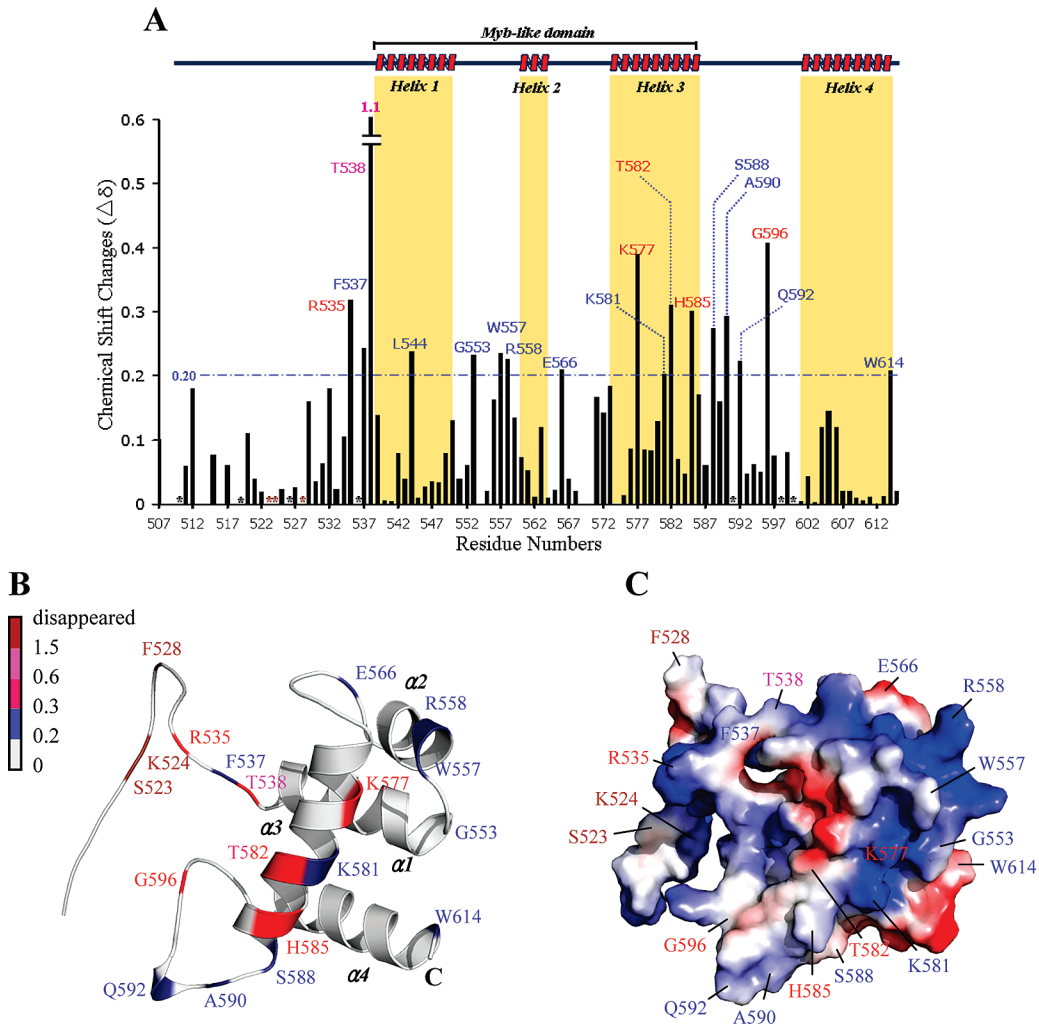

FIGURE 8: NMR chemical perturbation of $RTBP1_{506-615}$ upon binding to telomeric DNA. (A) Changes in the chemical shifts of $RTBP1_{506-615}$ induced by complex formation with telomeric DNA. Chemical shift changes were calculated as $\Delta\delta_{total} = [(\Delta\delta_{HN})^2 + (\Delta\delta_N/5)^2]^{1/2}$. The residues that exhibit chemical shift changes above 1 ppm, above 0.3 ppm, and between 0.2 and 0.3 ppm are colored pink, red, and blue, respectively. The resonance peaks of the amino acid residues that disappeared upon DNA binding are marked with a brown asterisk. Proline residues are marked with a black asterisk. The positions of the α-helices are indicated schematically at the top of the figure. (B) Ribbon diagram of $RTBP1_{506-615}$ indicating DNA binding residues. The DNA binding residues that exhibited chemical shift changes are colored pink, red, blue, and brown as described for panel A. (C) Electrostatic surface potentials of $RTBP1_{506-615}$. Surface residues are color-coded according to their charges (blue for positively charged, red for negatively charged, and white for neutral residues).

Table 3: DNA Interaction Comparison of $RTBP1_{506-615}$ and the DNA Binding Domains of Other Telomere Binding Proteins

	$RTBP1_{506-615}$	$NgTRF1_{561-681}$	$AtTRP1_{464-560}$	$hTRF1_{378-439}$
binding affinity	6.22×10^{-8} M	4.1×10^{-8} M	1.1×10^{-8} M	2.0×10^{-7} M
structural motif				
N-terminal arm	S523, K524, F528, R535, F537, T538	K567, S572, R575, R577, R578, F580	Q464, R465, R469	R380, Q381, W383
helix 1/helix 2	L544, G533, W557, R558, E556	R601, R614	G489	W403, S404, R415
helix 3	K577, K581, T582, H585	Y616, K620, D621, K622, K624, T629	R505, T506, K511, D512, K513, K515, T516, L517, H519, T520, A521, K522, I523	K421, D422, R423, R425
loop 3/helix 4	S588, A590, Q592, G596, W614	R638	R528, R529, G530, E531, V533	

in RTBP1 could be involved in DNA binding as well as stabilizing the structure through hydrophobic interactions with other parts of the molecule. As in other Myb motifs, helix 3 in RTBP1 functions as a sequence-specific recognition helix and the short N-terminal arm also interacts with the telomeric DNA.

A careful structural comparison of RTBP1 with other plant telomeric proteins revealed that RTBP1 more closely resembles NgTRF1 than AtTRP1, based on the orientation of helices (*26, 27*). The structural comparison between $RTBP1_{506-615}$ and $NgTRF1_{561-681}$ showed a high degree of homology in solution. However, it is not clear why the solution structures of $RTBP1_{506-615}$ and $AtTRP1_{464-560}$ are different in the absence of telomeric DNA. This structural deviation could be due to different experimental conditions and data analysis. Thus, further study will be required to examine whether the DNA binding domains of plant telomere binding proteins share similar backbone architecture in solution.

DNA bending by telomeric proteins such as hTRF1 and yeast Rap1 could induce the proper telomere structure which is required for their function (*42*). It is possible

that RTBP1 plays an architectural role in the plant telomere function, causing DNA bending and thus establishing and/or maintaining an active telomere configuration. Although a single RTBP1 binding to telomeric DNA introduces a minor distortion on DNA, clustered RTBP1 binding along the telomeric repeats could result in the folding back of the telomere itself. Recently, telomeric DNA in the plant *Pisum sativum* (garden pea) has been found arranged into telomere loops, proposed to sequester the telomere from unwanted DNA repair events (*46*). It is also possible that plants have evolved other mechanisms for capping their telomeres because approximately half of telomeres in *Arabidopsis* lack the single-stranded 3′-overhangs (*47*). The ability of RTBP1 to bend DNA could contribute to the overall configuration of the telomeric DNA.

In summary, in this study, we clarified the biochemical and structural features of the DNA binding domain of RTBP1, providing a molecular basis for DNA recognition by the telomere binding proteins, which are widespread in higher plants. We propose that RTBP1 plays an important role in telomere function by binding to and bending the DNA. The fourth helix of the Myb extension, a unique feature of plant telomere binding proteins, appears to be important for stabilizing the overall structure.

REFERENCES

1. Greider, C. W. (1996) Telomere length regulation. *Annu. Rev. Biochem. 65*, 337–365.
2. Smogorzewska, A., and de Lange, T. (2004) Regulation of telomerase by telomeric proteins. *Annu. Rev. Biochem. 73*, 177–208.
3. Blasco, M. A., Lee, H. W., Hande, M. P., Samper, E., Lansdorp, P. M., DePinho, R. A., and Greider, C. W. (1997) Telomere shortening and tumor formation by mouse cells lacking telomerase RNA. *Cell 91*, 25–34.
4. Richards, E. J., and Ausubel, F. M. (1988) Isolation of a higher eukaryotic telomere from *Arabidopsis thaliana*. *Cell 53*, 127–136.
5. Lingner, J., Cooper, J. P., and Cech, T. R. (1995) Telomerase and DNA end replication: No longer a lagging strand problem? *Science 269*, 1533–1534.
6. Autexier, C., and Lue, N. F. (2006) The structure and function of telomerase reverse transcriptase. *Annu. Rev. Biochem. 75*, 493–517.
7. Price, C. M., and Cech, T. R. (1987) Telomeric DNA-protein interactions of *Oxytricha* macronuclear DNA. *Genes Dev. 1*, 783–793.
8. Nugent, C. I., Hughes, T. R., Lue, N. F., and Lundblad, V. (1996) Cdc13p: A single-strand telomeric DNA-binding protein with a dual role in yeast telomere maintenance. *Science 274*, 249–252.
9. Baumann, P., and Cech, T. R. (2001) Pot1, the putative telomere end-binding protein in fission yeast and humans. *Science 292*, 1171–1175.
10. Shakirov, E. V., Surovtseva, Y. V., Osbun, N., and Shippen, D. E. (2005) The *Arabidopsis* Pot1 and Pot2 proteins function in telomere length homeostasis and chromosome end protection. *Mol. Cell. Biol. 25*, 7725–7733.
11. Kwon, C., and Chung, I. K. (2004) Interaction of an *Arabidopsis* RNA-binding protein with plant single-stranded telomeric DNA modulates telomerase activity. *J. Biol. Chem. 279*, 12812–12818.
12. Yoo, H. H., Kwon, C., Lee, M. M., and Chung, I. K. (2007) Single-stranded DNA binding factor AtWHY1 modulates telomere length homeostasis in *Arabidopsis*. *Plant J. 49*, 442–451.
13. van Steensel, B., and de Lange, T. (1997) Control of telomere length by the human telomeric protein TRF1. *Nature 385*, 740–743.
14. van Steensel, B., Smogorzewska, A., and de Lange, T. (1998) TRF2 protects human telomeres from end-to-end fusions. *Cell 92*, 401–413.
15. Griffith, J. D., Comeau, L., Rosenfield, S., Stansel, R. M., Bianchi, A., Moss, H., and de Lange, T. (1999) Mammalian telomeres end in a large duplex loop. *Cell 97*, 503–514.
16. Lustig, A. J., Kurtz, S., and Shore, D. (1990) Involvement of the silencer and UAS binding protein RAP1 in regulation of telomere length. *Science 250*, 549–553.
17. Cooper, J. P., Nimmo, E. R., Allshire, R. C., and Cech, T. R. (1997) Regulation of telomere length and function by a Myb-domain protein in fission yeast. *Nature 385*, 744–747.
18. Chen, C. M., Wang, C. T., and Ho, C. H. (2001) A plant gene encoding a Myb-like protein that binds telomeric GGTTAG repeats in vitro. *J. Biol. Chem. 276*, 16511–16519.
19. Hwang, M. G., Chung, I. K., Kang, B. G., and Cho, M. H. (2001) Sequence-specific binding property of *Arabidopsis thaliana* telomeric DNA binding protein 1 (AtTBP1). *FEBS Lett. 503*, 35–40.
20. Hwang, M. G., and Cho, M. H. (2007) *Arabidopsis thaliana* telomeric DNA-binding protein 1 is required for telomere length homeostasis and its Myb-extension domain stabilizes plant telomeric DNA binding. *Nucleic Acids Res. 35*, 1333–1342.
21. Karamysheva, Z. N., Surovtseva, Y. V., Vespa, L., Shakirov, E. V., and Shippen, D. E. (2004) A C-terminal Myb Extension Domain Defines a Novel Family of Double-strand Telomeric DNA-binding Proteins in *Arabidopsis*. *J. Biol. Chem. 279*, 47799–47807.
22. Yang, S. W., Kim, D. H., Lee, J. J., Chun, Y. J., Lee, J. H., Kim, Y. J., Chung, I. K., and Kim, W. T. (2003) Expression of the telomeric repeat binding factor gene NgTRF1 is closely coordinated with the cell division program in tobacco BY-2 suspension culture cells. *J. Biol. Chem. 278*, 21395–21407.
23. Yang, S. W., Kim, S. K., and Kim, W. T. (2004) Perturbation of NgTRF1 expression induces apoptosis-like cell death in tobacco BY-2 cells and implicates NgTRF1 in the control of telomere length and stability. *Plant Cell 16*, 3370–3385.
24. Hong, J. P., Byun, M. Y., Koo, D. H., An, K., Bang, J. W., Chung, I. K., An, G., and Kim, W. T. (2007) Suppression of rice telomere binding protein 1 results in severe and gradual developmental defects accompanied by genome instability in rice. *Plant Cell 19*, 1770–1781.
25. Nishikawa, T., Okamura, H., Nagadoi, A., König, P., Rhodes, D., and Nishimura, Y. (2001) Solution structure of a telomeric DNA complex of human TRF1. *Structure 9*, 1237–1251.
26. Sue, S. C., Hsiao, H. H., Chung, B. C., Cheng, Y. H., Hsueh, K. L., Chen, C. M., Ho, C. H., and Huang, T. H. (2006) Solution structure of the *Arabidopsis thaliana* telomeric repeat-binding protein DNA binding domain: A new fold with an additional C-terminal helix. *J. Mol. Biol. 356*, 72–85.
27. Ko, S., Jun, S. H., Bae, H., Byun, J. S., Han, W., Park, H., Yang, S. W., Park, S. Y., Jeon, Y. H., Cheong, C., Kim, W. T., Lee, W., and Cho, H. S. (2008) Structure of the DNA-binding domain of NgTRF1 reveals unique features of plant telomere-binding proteins. *Nucleic Acids Res. 36*, 2739–2755.
28. Yu, E. Y., Kim, S. E., Kim, J. H., Ko, J. H., Cho, M. H., and Chung, I. K. (2000) Sequence-specific DNA recognition by the Myb-like domain of plant telomeric protein RTBP1. *J. Biol. Chem. 275*, 24208–24214.
29. Thompson, J. F., and Landy, A. (1988) Empirical estimation of protein-induced DNA bending angles: Applications to lambda site-specific recombination complexes. *Nucleic Acids Res. 16*, 9687–9705.
30. Bodenhausen, G., and Ruben, D. J. (1980) Natural Abundance Nitrogen-15 NMR by Enhanced Heteronuclear Spectroscopy. *Chem. Phys. Lett. 69*, 185–189.
31. Vuister, G. W., and Bax, A. (1992) Resolution enhancement and spectral editing of uniformly ^{13}C-enriched proteins by homonuclear broadband ^{13}C decoupling. *J. Magn. Reson. 98*, 428–435.
32. Grzesiek, S., Dobeli, H., Gentz, R., Garotta, G., Labhardt, A. M., and Bax, A. (1992) ^{1}H, ^{13}C, and ^{15}N NMR backbone assignments and secondary structure of human interferon-γ. *Biochemistry 31*, 8180–8190.
33. Grzesiek, S., and Bax, A. (1992) Correlating Backbone Amide and Side Chain Resonances in Larger Proteins by Multiple Relayed Triple Resonance NMR. *J. Am. Chem. Soc. 114*, 6291–6293.
34. Vuister, G. W., and Bax, A. (1994) Measurement of four-bond HN-Hα J-couplings in staphylococcal nuclease. *J. Biomol. NMR 4*, 193–200.
35. Grzesiek, S., and Bax, A. (1993) Amino acid type determination in the sequential assignment procedure of uniformly ^{13}C/^{15}N-enriched proteins. *J. Biomol. NMR 3*, 185–204.

36. Kay, L., Keifer, P., and Saarinen, T. (1992) Pure absorption gradient enhanced heteronuclear single quantum correlation spectroscopy with improved sensitivity. *J. Am. Chem. Soc. 114*, 10663–10665.
37. Kay, L. E., Xu, G. Y., Singer, A. U., Muhandiram, D. R., and Formankay, J. D. (1993) A gradient-enhanced HCCH-TOCSY experiment for recording side-chain ^{1}H and ^{13}C correlations in H_2O samples of proteins. *J. Magn. Reson., Ser. B 101*, 333–337.
38. Davis, A. L., Keeler, J., Laue, E. D., and Moskau, D. (1992) Experiments for recording pure absorption heteronuclear correlation spectra using pulsed field gradients. *J. Magn. Reson. 98*, 207–216.
39. Pervushin, K., Riek, R., Wider, G., and Wuthrich, K. (1997) Attenuated T2 relaxation by mutual cancellation of dipole-dipole coupling and chemical shift anisotropy indicates an avenue to NMR structures of very large biological macromolecules in solution. *Proc. Natl. Acad. Sci. U.S.A. 94*, 12366–12371.
40. Guntert, P. (2004) Automated NMR structure calculation with CYANA. *Methods Mol. Biol. 278*, 353–378.
41. König, P., Fairall, L., and Rhodes, D. (1998) Sequence-specific DNA recognition by the myb-like domain of the human telomere binding protein TRF1: A model for the protein-DNA complex. *Nucleic Acids Res. 26*, 1731–1740.
42. Bianchi, A., Smith, S., Chong, L., Elias, P., and de Lange, T. (1997) TRF1 is a dimer and bends telomeric DNA. *EMBO J. 16*, 1785–1794.
43. Ko, S. G., Shin, J., Yu, E. Y., Chung, I. K., Tanaka, T., and Lee, W. (2003) ^{1}H, ^{13}C and ^{15}N resonance assignments of rice telomere binding domain from *Oryza sativa*. *J. Biomol. NMR 27*, 89–90.
44. Konig, P., Giraldo, R., Chapman, L., and Rhodes, D. (1996) The crystal structure of the DNA-binding domain of yeast RAP1 in complex with telomeric DNA. *Cell 85*, 125–136.
45. Tanikawa, J., Yasukawa, T., Enari, M., Ogata, K., Nishimura, Y., Ishii, S., and Sarai, A. (1993) Recognition of specific DNA sequences by the c-myb protooncogene product: Role of three repeat units in the DNA-binding domain. *Proc. Natl. Acad. Sci. U.S.A. 90*, 9320–9324.
46. Cesare, A. J., Quinney, N., Willcox, S., Subramanian, D., and Griffith, J. D. (2003) Telomere looping in *P. sativum* (common garden pea). *Plant J. 36*, 271–279.
47. Riha, K., McKnight, T. D., Fajkus, J., Vyskot, B., and Shippen, D. E. (2000) Analysis of the G-overhang structures on plant telomeres: Evidence for two distinct telomere architectures. *Plant J. 23*, 633–641.

BI801270G